ON THE PARTICULATE MODELING OF SOIL-FLUID INTERACTION IN GEOTECHNICAL ENGINEERING

Nahid Salem[1], Mohamed A. Meguid[2]

[1]Graduate Student, Civil Engineering and Applied Mechanics, McGill University, Canada

[2] Associate professor, Civil Engineering and Applied Mechanics, McGill University, Canada

Department of Civil Engineering and Applied Mechanics – McGill University, Montreal, QC, Canada

ABSTRACT

Fluid-particle interaction is an important subject that can be applied to a variety of domains including sediments analysis, material processing, and petroleum engineering. It is also used in geotechnical applications to model seepage, soil erosion, sand pile formation, and flow under sheet pile walls. Recent advances in computational power allowed for the development of more enhanced constitutive models that are capable of analyzing the interaction forces between particles, as well as between particles and fluids. Extensive research is needed to further understand this coupled behavior and the associated particle-fluid motion at the microscale level. This study evaluates the available experimental and theoretical methods used by researchers to measure and calculate soil-fluid interaction applied to geotechnical engineering. Emphasis is placed on coupled discrete element-computational fluid dynamics approaches as they are able to capture the discrete nature of the granular material as well as the continuum nature of the fluid. A simple example will be used to illustrate the advantages of the method and describe the initiation of particle movement and the relationship between micro and macro material parameters required for the analysis.

Keywords: Soil-fluid interaction; discrete element; coupled analysis; granular material.

L'interaction entre les fluides et les particules est un sujet important qui peut s'appliquer à divers domaines, y compris l'analyse des sédiments, le traitement des matériaux et l'ingénierie du pétrole. Il est également utilisé dans des applications géotechniques pour modéliser les infiltrations, l'érosion des sols, la formation de pieux de sable et l'écoulement sous les parois des tas. Les progrès récents en termes de puissance de calcul ont permis le développement de modèles constitutifs plus améliorés qui sont capables d'analyser les forces d'interaction entre les particules, ainsi qu'entre les particules et les fluides. Des recherches approfondies sont nécessaires pour mieux comprendre ce comportement couplé et le mouvement des particules-fluides associé au niveau des micro-échelles. Cette étude évalue les méthodes expérimentales et théoriques disponibles utilisées par les chercheurs pour mesurer et calculer l'interaction sol-fluide appliquée à l'ingénierie géotechnique. L'accent est mis sur les approches associées à la dynamique des fluides de l'élément discret, car elles sont capables de capturer la nature discrète du matériau granulaire ainsi que la nature continue du fluide. Un exemple simple sera utilisé pour illustrer les avantages de la méthode et décrire l'initiation du mouvement des particules et la relation entre les paramètres micro et macro-matériaux requis pour l'analyse.

Mots-clés: interaction sol-fluide; Élément discret; Analyse couplée; Matériel granulaire.

1 INTRODUCTION

Soil erosion is a global problem that has effects on several domains such as agriculture, ecology, and land surface changes. It causes great losses of resources. From a civil engineering perspective, and more specifically geotechnical soil erosion, erosion can negatively affect the performance of structure foundations. This is particularly problematic in earth structures which may fail due to piping. It is estimated by (Fell et al, 2003; Foster et al., 2000) 50% of embankment dam failure occurs due to this phenomena. The hydraulic gradient across the foundation mobilizes particles and transports them. Over time, the collective movement of soil particles leads to the formation of interconnecting pipes through the foundation that eventually leads to breaching of the structure. A main problem of piping failure is that it often develops rapidly, and only exhibits signs of failure after the failure has already progressed inside the structure.

In order to prevent or mitigate internal erosion and to be able to quantify the associated risk imposed on geotechnical structures, a fundamental understanding of soil-water behavior is needed. Some of the main aspects of particle-fluid flow include velocity, structure, and forces. Velocity has been extensively studied at the macroscale level, however, with recent advances in computational power, the micro mechanical behavior of soil can also be studied.

Previous studies have focused on the macroscopic behavior of soil and has been studied theoretically and experimentally. This helped identify the different stages of the piping phenomena: initiation, progression, boil formation and total heave. The effect of confining pressure, hydraulic gradient, and seepage forces have

previously been investigated using these methods (Tao et al, 2017). With advances in high performance computing, numerical models have helped provide quantitative data and shed light into the micro mechanical behavior of soil during piping. Previous numerical models focused on modeling soil behavior through a pure discrete element method (DEM). More recently, coupled models have the ability to capture the behavior of both solid soil particles through the DEM and the fluid behavior using computational fluid dynamics (CFD). A fully coupled CFD-DEM model is used in this paper to study the progression of piping in soil. The model set up and parameters are presented in the methodology section. The particle velocities and the void fractions throughout the sample are presented and discussed in the following Results section.

2 METHODOLOGY

2.1 Governing Equations

As mentioned, the coupled soil-fluid behavior is studied in this paper using the coupled CFD-DEM method. This has originally been proposed by (Tsuji et al, 1992). This method allows for the particle-fluid interaction to be captured by making use of the current development in computational power. The coupling of the discrete-continuum algorithm is done through two open source software packages: LIGGGHTS and OpenFOAM (Kloss et al, 2010; Kloss et al, 2012. The former is based on a molecular dynamics simulator with improved general granular and granular heat transfer simulation. OpenFOAM on the other hand is capable of solving complex fluid flow problems that involve turbulence, heat transfer and solid dynamics, as well as electromagnetics. Both softwares could run in parallel.

The LIGGGHTS software, particle motion is governed by Newton's second law of motion. Equations [1] and [2] below describe the translational and rotational motion of a particle

$$m_p \frac{dvp}{dt} = f_p^g + \Sigma f_p^c + f_p^f \quad [1]$$

$$I_p \frac{dwp}{dt} = \Sigma M_p \quad [2]$$

where vp and wp are the translational and angular velocities of particle p, f_p^g is the gravitational force; f_p^c is the contact force on particle p at contact point c; and f_p^f the particle–fluid interaction force acting on particle p by fluid phase. In the OpenFOAM software, fluid behavior is governed by Navier-Stokes law of conservation of mass and momentum with respect to locally averaged variables. Equation [3] below describes conservation of mass and equation [4] describes conservation of momentum.

$$\frac{dn}{\partial t} + \nabla.\left(nv_f\right) = 0 \quad [3]$$

$$\rho_f \left(\frac{\partial(nv_f)}{\partial t} + \nabla.(\mathrm{n}v_f v_f)\right) = -\mathrm{n}\nabla p_f \mathrm{I} + \mathrm{n}\nabla.\tau\text{-}f_f^p + n\rho_f f_g \quad [4]$$

where n is porosity; v_f avg. fluid velocity p, p_f is the gravitational force; $\nabla.$ is the gradient operator; τ is the stress tensor of the fluid; I is the identity tensor of the fluid; and f_p^f the average interaction force vector by the particles on the fluid phase; $\mathrm{f_g}$ is the gravitational acceleration vector.

The coupling is done by exchanging data between the two packages during computation. The particle data such as particle position, velocity, and particle size is sent from LIGGGHTS to the OpenFoam solver. Flow data, such as flow velocity and pressure is transferred to LIGGGHTS. The exchange of particle interaction forces, drag forces $\boldsymbol{F}^d$ and buoyancy forces $\boldsymbol{F}^b$ are the core components of the coupling. The expression for these forces is shown in [5] and [6].

$$\boldsymbol{F}^d = \frac{1}{8} C_d \varrho \pi d_p^2 (\boldsymbol{U}^f - \boldsymbol{U}^p)\left|\boldsymbol{U}^f - \boldsymbol{U}^p\right| \varepsilon^{1-x} \quad [5]$$

$$\boldsymbol{F}^b = \frac{1}{6} = \pi \varrho d_p^3 g \quad [6]$$

where C_d is the particle fluid drag coefficient, d_p is the particle diameter, and ε^{1-x} is a corrective term to account for the effect of the surrounding particles. x is shown in expression [7] below.

$$\chi = 3.7 - 0.65\exp[-\frac{\left(1.5 - log_{10}Re_p\right)^2}{2}] \quad [7]$$

While it is preferred that the exchange of information of the interaction forces is done after every step of the DEM and the CFD model, this is unnecessarily computationally demanding. Accuracy and efficiency can be achieved by exchanging information for every CFD time step, after every 100 DEM time steps, as also indicated by Zhao et al. (2013).

2.2 Model Set up

A 3D coupled CFD-DEM piping erosion model similar to that of the experimental set up reported by (Fleshman & Rice, 2014) is used. The aim of this experiment was to study the mechanisms of piping erosion in sandy soil. This was done by measuring the hydraulic conditions of a soil sample subjected to a vertical flow. A uniform hydraulic gradient is applied and the mechanisms of piping are observed. The sample set up for the numerical model is shown in Figure 1 below. The cylinder sample has a diameter of 3 cm and a height of 1.4 cm is filled by the particles. The CFD domain has an abundant height up to 5.5 cm is to allow the particles to move upwards freely. Sand particles are modeled as perfect spheres and friction between particles is considered. While the average values of Young's modulus from literature review is in the range of 10^6 to 10^9 Pa (Belheine et al, 2009; Zhou et al. 2010, Zhao et al., 2013). However, in this study 10^6 Pa are used to allow for a larger time step. This

is acceptable as it has been demonstrated by (Chand et al, 2012) that this does not significantly affect the results.

Other parameters are similar to the ones used by (van Buijtenen, 2011). However, the time steps have been modified to suit this model. Also, the effect of different particle sizes was investigated by running the model for two cases, Case 1 with 1 mm diameter, and Case 2 with 0.5 mm diameter. The details of the parameters are shown in Table 1 below.

Table 1. Simulation Set up parameters

Characteristics	
Particle Shape	Sphere
Particles Density	2650 kg/m^3
Fluid Density	1000 kg/m^3
Particle Diameter (Case 1)	1 mm
Particle Diameter (Case 2)	0.5 mm
Restitution coefficient	0.2
Friction coefficient	0.5
Young's modulus	5x10^6 Pa
Simulation time	10 s
Poisson ratio	0.3
Viscosity	1x10^{-6} m^2/s
DEM Time step	1x 10^{-5} s
CFD Time step	1x 10^{-4} s
Gravity	9.8 m/s^s

The progression of particle velocities and void fraction for the setup is discussed in section 3 below. As the behavior of the particles is different at different layers of the soil, for the average void fraction the results are shown for a representative collection of particles from both the upper and lower levels. The location of lower particles is shown in Figure 1 below and the location of the upper particles is shown in Figure 2 below.

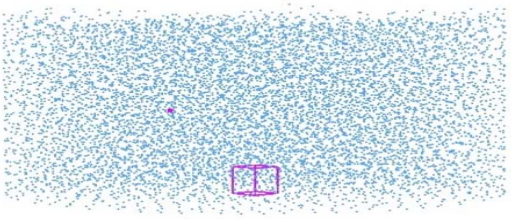

Figure 1 Location of Lower Particles selected for results

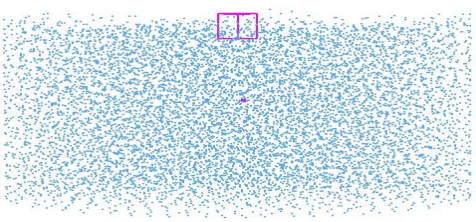

Figure 2 Location of Upper Particles selected for results

3 RESULTS AND DISCUSSION

3.1 Case 1: Progression of Particle Velocities and Void Fraction

The CFD-DEM model used in this simulation exhibits the behavior of the soil particles as time passes. There are driving and resisting forces that affect particle motion. Driving forces acting are drag forces, viscous shear forces, and pressure gradient forces. Resistive forces acting are gravity, interparticle friction, interparticle interaction, and particle wall friction. Particle motion starts to occur when the driving forces exceed the resistive forces. Figure 3 below shows the velocities of the particles at times 1s, 3s, 6s, and 10s at the end of the simulation. Initially particles at the surface of the sample move at larger velocities. This is because there are no particles above that restrict their motion. Furthermore, it is observed that initially there are fluctuations in particle velocities of the top layer.

As time progresses, these fluctuations decrease. Previous experimental studies on piping such as the one conducted by (Fleshman & Rice, 2014) describe the stages of piping as: first visible movement, heave progression, boil formation, and total heave. The fluctuations in velocities of the particles in the top layer may indicate the initiation stage. While boil formation was not observed in this numerical model, the velocities of particles increase over time indicating the progression of erosion. As can be seen at the final stage (d) 10s the velocity of most of the particles is 0.616 cm/s compared to stage (b) 3s where the velocity of most of the particles is 0.00459 cm/s. This increase in velocity lead to the rise of all soil particles in the sample. As the particles start to move, the positions of the particles change causing local rearrangement of particles. This in turn leads to changes in the local void ratio. The results are demonstrated below. The average void ratio of a group of particles from both the upper layer is shown in Figure 4 and the for the lower layer of the sample are shown in Figure 5.

For the upper layer of the sample, the void ratio decreased from 1 to 0.866 in the first second. This large void ratio leads to lower hydraulic forces. The void ratio then continues to decrease, stabilize, then decrease again over the remaining 9 seconds. It is expected that the upward seepage would loosen the soil particles. From the video generated for this simulation, overall the upward flow dilates the soil. As the soil particles begin moving, the void fraction increases leading to smaller hydraulic forces.

In the lower layer of the sample, the average void ratio after 1 s is 0.356 which is much lower than that of the upper layer (0.866). This indicates stronger hydraulic forces at the lower layer, which is consistent with lower velocities at the bottom layer throughout the simulation. This is because the lower layer is subjected to the forces of all the particles above it. The average void ratio then slowly increases back to 0.4 over the remaining 9 seconds. This may be due to particle rearrangement

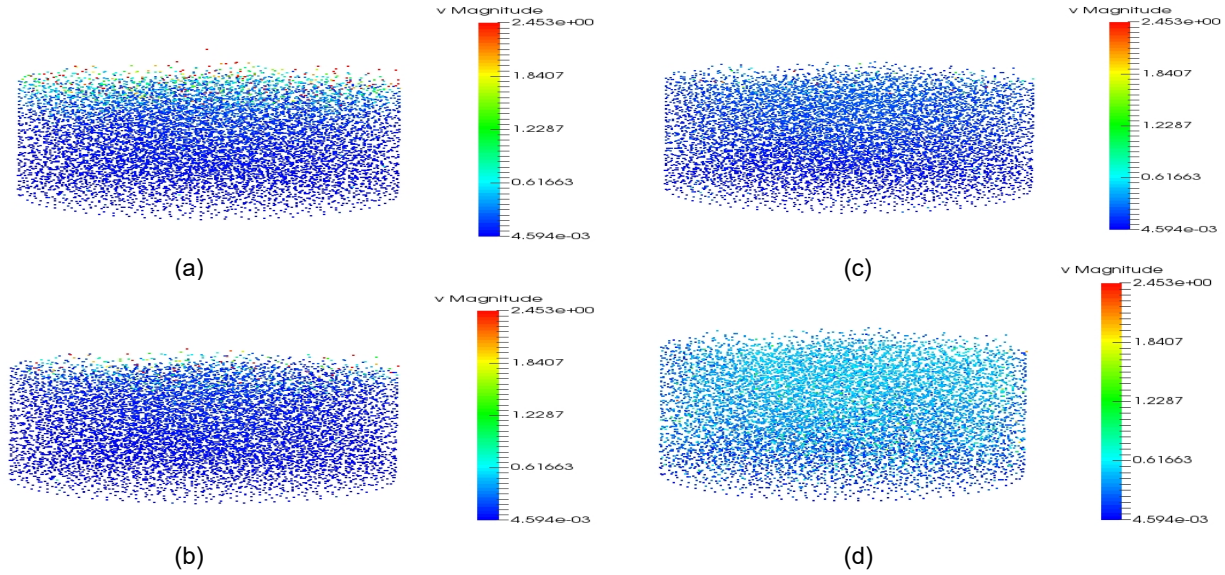

Figure 3 Progression of Particle Velocities (Case 1)

occurring at the bottom of the sample. Throughout the sample, as time passes, the flow velocity begins to increase and the initial equilibrium stage begins to be broken. The flow is uniform and follows Darcy's law. Since the particles at the surface have the lowest contact forces initially, the breakage of the equilibrium starts to occur at the surface. This leads to particle movement, and rearrangement, which leads to a larger void ratio and lower hydraulic forces. It then continues to progress throughout the sample until the particles at all layers move.

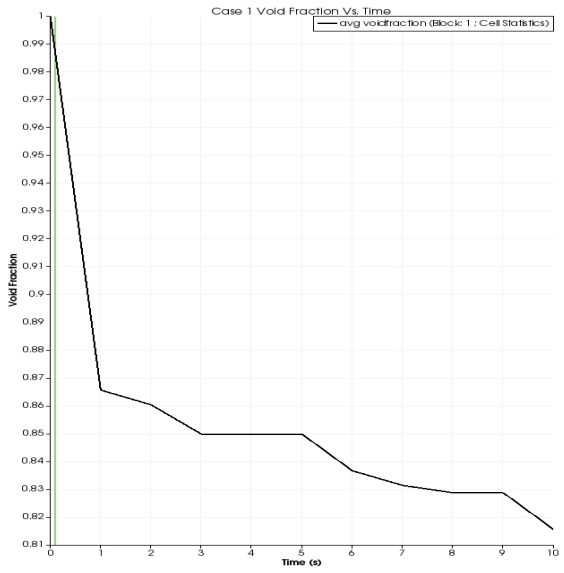

Figure 4 Case 1 Void Ratio (Upper Layer)

1.1 Case 2 Progression of Particle Velocities and Void Fraction

The same model is run for particles with half the diameter to study the effect of particle size. Similar patterns are observed with case 1 for the progression of particle velocities over time as shown in Figure 8. The particles at the surface begin to move, particles begin to rearrange, and over time the velocities of particles at all layers of the sample increases. This is expected as all other parameters were kept the same. However, in this case in the initial stage, more particles at the surface exhibited higher velocities in the range between 2.45 cm/s and 1.23 cm/s. compared to particles between 2.45 cm/s and 1.84 cm/s. It is clear that particle movement occurs much faster for finer particles than for the larger particles.

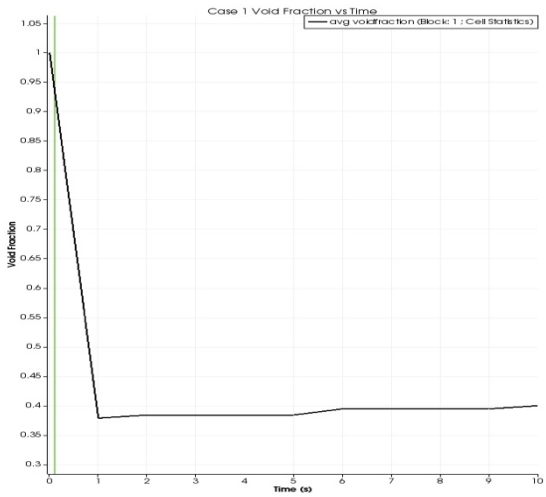

Figure 5 Case 1 Void Ratio (Lower Layer)

In addition, similar patterns are observed for the changes in the average void ratio over time in both the upper and lower layers of the sample. In the upper layer, the changes in the void ratio decrease from 1 to 0.866 in the first second, and continues to decrease over stages in the remaining 9 seconds as shown in Figure 6. However, a difference is observed in the void fraction of the lower layer, where the void fraction drops to 0 after the first second. This is demonstrated in Figure 7 below. It remains zero and only increases slightly to 0.03 at 10 seconds. This may be due to particle rearrangement at the bottom of the sample as in the previous case.

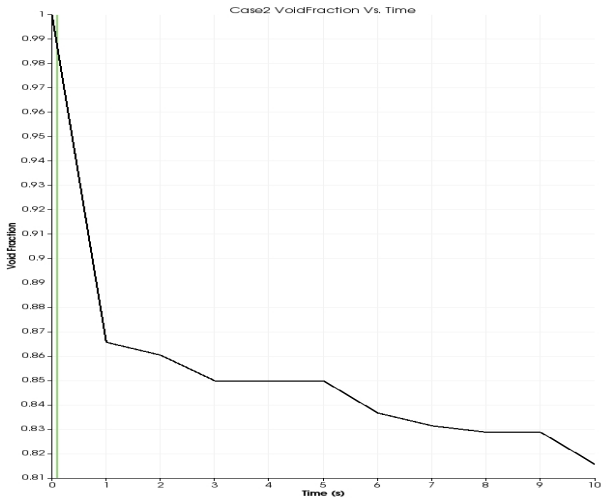

Figure 6 Case 2 Void Ratio (Upper Layer)

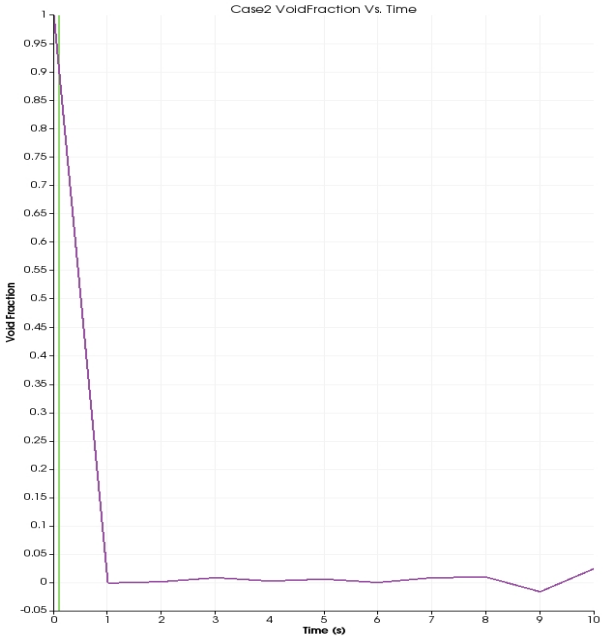

Figure 7 Case 2 Void Ratio (Lower Layer)

4. CONCLUSION

This paper models the behavior of soil during the piping process using a coupled CFD to model the fluid behavior, and DEM to model the solid particles behavior. The model is conducted on particles of 1 mm and 0.50 mm diameters, with parameters of sandy soil. The different stages during piping is observed for both cases, as well as changes in the void ratio in the upper and lower layer of the soil sample. Three main stages are observed in the results: initiation, progression, and heave. These stages have been confirmed experimentally as reported by (Fleshman & Rice, 2014). A sand boil stage was observed in the experimental study, that was not identified in the numerical model. This may be because the experimental model is relatively larger than the numerical model.

Despite that, CFD-DEM coupled numerical models are considered a powerful tool that provides quantitative data at the particle scale that is difficult to be obtained experimentally. In this paper, the quantitative changes in particle velocity and void ratio are demonstrated. In addition, this tool can be used for further analysis such as porosity and local contact forces and their orientations at different length and time scales. However, the time step is considered a limitation in this study. Both the CFD and DEM time step are selected to allow for an accurate numerical converging of the results. This depends on the particle properties. In this study, a lower modulus of particles is selected to allow for a larger time step to be used. Since the same parameters are used in the models of both Case 1 and Case 2, the errors would apply to both. However, further studies are needed to establish this effect. While this study sheds some light into the micromechanical behavior of soil during piping, further analysis of different parameters in future models will allow a better understanding of this mechanism which is still not fully understood.

Acknowledgement

This research is supported by the Natural Sciences and Engineering Research Council of Canada (NSERC). Financial support provided by McGill Engineering Doctoral Award (MEDA) to the first author is appreciated.

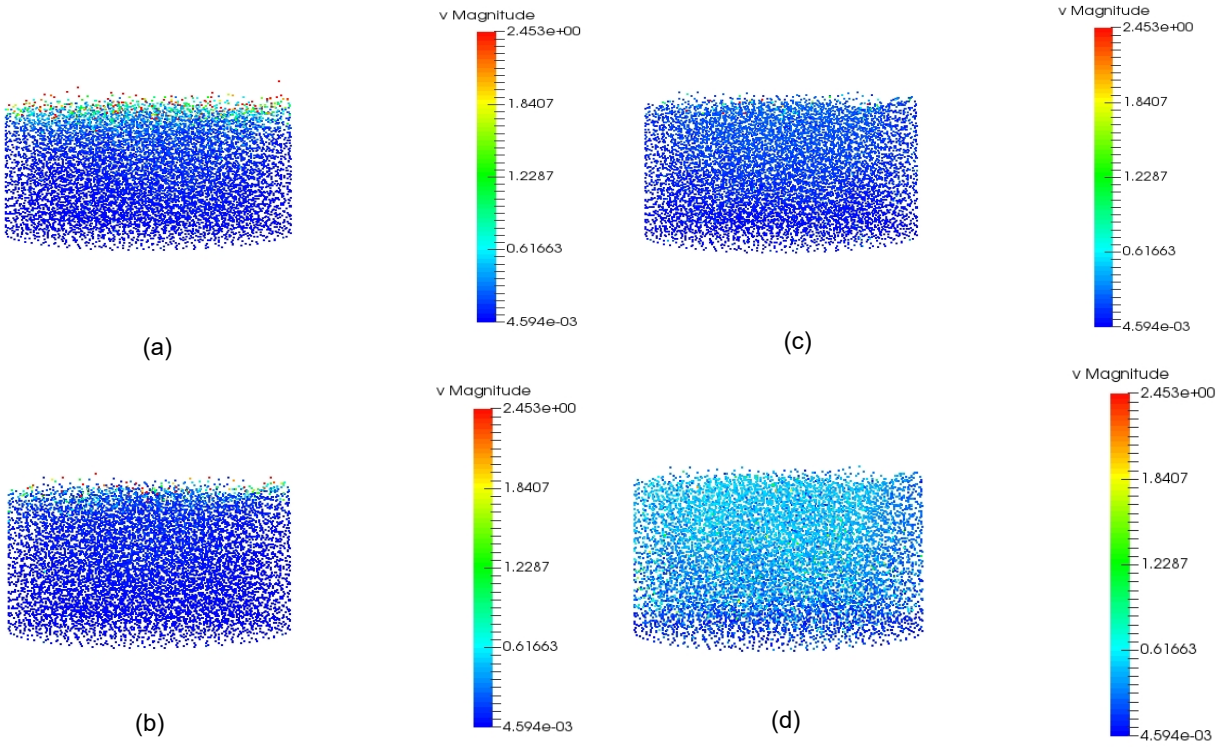

Figure 8 Progression of Particle Velocities (Case 2)

5. REFERENCES

Belheine N,PlassiardJP,Donze´FV,DarveF,SeridiA(2009) Numerical simulation of drained triaxial test using 3D discrete element modeling. Comput Geotech 36:320–331

Chand R, Khaskheli MA, Qadir A, Ge B, Shi Q (2012) Discrete particle simulation of radial segregation in horizontally rotating drum: effects of drum-length and non-rotating end-plates. Phys A 391(40):4590–4596

Fleshman, M. S., & Rice, J. D. (2014). Laboratory modeling of the mechanisms of piping erosion initiation. Journal of Geotechnical and Geoenvironmental Engineering (ASCE), 140(6), 04014017

Fell R, Wan CF (2003) Time for development of internal erosion and piping in embankment dams. J Geotech Geoenviron 129(4):307–314

Foster MA, Fell R, Spannagle M (2000) A method for estimating the relative likelihood of failure of embankment dams by internal erosion and piping. Can Geotech J 37(5):1025–1061

Kloss C, Goniva C. LIGGGHTS-A new open source discrete element simulation software. In: Proceedings of 5th international conference on discrete element methods, pp 25–26, London. ISBN 978-0-9551179-8-5, 2010

Kloss C, Goniva C, Hager A, Amberger S, Pirker S (2012) Models, algorithms and validation for opensource DEM and CFD-DEM. Progr Comput Fluid Dyn Int J 12(2–3):140–152

Leadbeater T, Parker DJ (2011) Numerical and experimental study on multiple-spout fluidized beds. Chem Eng Sci 66(11):2368–2376

OpenFOAM. http://www.openfoam.com/

Tao, H., & Tao, J. Quantitative analysis of piping erosion micro-mechanisms with coupled CFD and DEM method. Acta Geotechnica, 1-20.

Zhao J, Shan T (2013) Coupled CFD–DEM simulation of fluid– particle interaction in geomechanics. Powder Technol 239:248–258

Zhou ZY, Kuang SB, Chu KW, Yu AB (2010) Discrete particle simulation of particle–fluid flow: model formulations and their applicability. J Fluid Mech 661:482–510